

# AMADEUS - The Acoustic Neutrino Detection Test System of the Deep-Sea ANTARES Neutrino Telescope

J.A. Aguilar, Imen Al Samarai, A. Albert, M. Anghinolfi, G. Anton, S. Anvar, M. Ardid, A.C. Assis Jesus, T. Astraatmadja, J.-J. Aubert, et al.

## ▶ To cite this version:

J.A. Aguilar, Imen Al Samarai, A. Albert, M. Anghinolfi, G. Anton, et al.. AMADEUS - The Acoustic Neutrino Detection Test System of the Deep-Sea ANTARES Neutrino Telescope. Nuclear Instruments and Methods in Physics Research Section A: Accelerators, Spectrometers, Detectors and Associated Equipment, 2010, 626-627, pp.128-143. 10.1016/j.nima.2010.09.053 . in2p3-00474914

# HAL Id: in2p3-00474914 https://in2p3.hal.science/in2p3-00474914v1

Submitted on 21 Apr 2010

**HAL** is a multi-disciplinary open access archive for the deposit and dissemination of scientific research documents, whether they are published or not. The documents may come from teaching and research institutions in France or abroad, or from public or private research centers.

L'archive ouverte pluridisciplinaire **HAL**, est destinée au dépôt et à la diffusion de documents scientifiques de niveau recherche, publiés ou non, émanant des établissements d'enseignement et de recherche français ou étrangers, des laboratoires publics ou privés.

# AMADEUS - The Acoustic Neutrino Detection Test System of the Deep-Sea ANTARES Neutrino Telescope

```
J.A. Aguilar <sup>a</sup>, I. Al Samarai <sup>b</sup>, A. Albert <sup>c</sup>, M. Anghinolfi <sup>d</sup>,
          G. Anton <sup>e</sup>, S. Anvar <sup>f</sup>, M. Ardid <sup>g</sup>, A.C. Assis Jesus <sup>h</sup>,
T. Astraatmadja h,1, J-J. Aubert b, R. Auer e, E. Barbarito i, B. Baret j,
 S. Basa k, M. Bazzotti l, W. Bertin b, S. Biagi l, M. C. Bigongiari a,
     M. Bou-Cabo <sup>g</sup>, M.C. Bouwhuis <sup>h</sup>, A. Brown <sup>b</sup>, J. Brunner <sup>b,2</sup>,
         J. Busto<sup>b</sup>, F. Camarena<sup>g</sup>, A. Capone<sup>n,o</sup>, C.Cârloganu<sup>p</sup>,
        G. Carminati <sup>l,m</sup>, J. Carr <sup>b</sup>, B. Cassano <sup>i</sup>, E. Castorina <sup>q,r</sup>,
        V. Cavasinni q,r, S. Cecchini m,s, A. Ceres i, Ph. Charvis t,
      T. Chiarusi <sup>m</sup>, N. Chon Sen <sup>c</sup>, M. Circella <sup>i</sup>, R. Coniglione <sup>u</sup>,
H. Costantini <sup>d</sup>, N. Cottini <sup>v</sup>, P. Coyle <sup>b</sup>, C. Curtil <sup>b</sup>, G. De Bonis <sup>n,o</sup>,
   M.P. Decowski h, I. Dekeyser w, A. Deschamps t, C. Distefano u,
          C. Donzaud j,x, D. Dornic b,a, D. Drouhin c, T. Eberl e,
        U. Emanuele <sup>a</sup>, J-P. Ernenwein <sup>b</sup>, S. Escoffier <sup>b</sup>, F. Fehr <sup>e</sup>,
V. Flaminio ^{q,r}, U. Fritsch ^{e}, J-L. Fuda ^{w}, P. Gay ^{p}, G. Giacomelli ^{\ell,m}.
   J.P. Gómez-González a, K. Graf e, G. Guillard y, G. Halladjian b,
       G. Hallewell b, H. van Haren Z, A.J. Heijboer h, E. Heine h,
         Y. Hello <sup>t</sup>, J.J. Hernández-Rey <sup>a</sup>, B. Herold <sup>e</sup>, J. Hößl <sup>e</sup>,
        M. de Jong h,1, N. Kalantar-Nayestanaki aa, O. Kalekin e,
 A. Kappes <sup>e</sup>, U. Katz <sup>e</sup>, P. Keller <sup>b</sup>, P. Kooijman <sup>h,ab,ac</sup>, C. Kopper <sup>e</sup>,
     A. Kouchner<sup>j</sup>, W. Kretschmer<sup>e</sup>, R. Lahmann<sup>e,*</sup>, P. Lamare<sup>f</sup>,
      G. Lambard b, G. Larosa g, H. Laschinsky e, H. Le Provost f,
        D. Lefèvre w, G. Lelaizant b, G. Lim h,ac, D. Lo Presti ad,
         H. Loehner <sup>aa</sup>, S. Loucatos <sup>v</sup>, F. Louis <sup>f</sup>, F. Lucarelli <sup>n,o</sup>,
               S. Mangano a, M. Marcelin k, A. Margiotta \ell, m,
J.A. Martinez-Mora g, A. Mazure k, M. Mongelli, T. Montaruli, ae,
M. Morganti q,r, L. Moscoso v,j, H. Motz e, C. Naumann v, M. Neff e,
        R. Ostasch<sup>e</sup>, D. Palioselitis<sup>h</sup>, G.E. Păvălaș<sup>af</sup>, P. Payre<sup>b</sup>,
J. Petrovic <sup>h</sup>, N. Picot-Clemente <sup>b</sup>, C. Picq <sup>v</sup>, V. Popa <sup>af</sup>, T. Pradier <sup>y</sup>,
   E. Presani h, C. Racca c, A. Radu af, C. Reed b,h, G. Riccobene u,
```

C. Richardt <sup>e</sup>, M. Rujoiu <sup>af</sup>, M. Ruppi <sup>i</sup>, G.V. Russo <sup>ad</sup>, F. Salesa <sup>a</sup>, P. Sapienza <sup>u</sup>, F. Schoeck <sup>e</sup>, J-P. Schuller <sup>v</sup>, R. Shanidze <sup>e</sup>, F. Simeone <sup>o</sup>, M. Spurio <sup>ℓ,m</sup>, J.J.M. Steijger <sup>h</sup>, Th. Stolarczyk <sup>v</sup>, M. Taiuti <sup>ag,d</sup>, C. Tamburini <sup>w</sup>, L. Tasca <sup>k</sup>, S. Toscano <sup>a</sup>, B. Vallage <sup>v</sup>, V. Van Elewyck <sup>j</sup>, G. Vannoni <sup>v</sup>, M. Vecchi <sup>n</sup>, P. Vernin <sup>v</sup>, G. Wijnker <sup>h</sup>, E. de Wolf <sup>h,ac</sup>, H. Yepes <sup>a</sup>, D. Zaborov <sup>ah</sup>, J.D. Zornoza <sup>a</sup>, J. Zúñiga <sup>a</sup>

```
<sup>à</sup>IFIC - Instituto de Física Corpuscular, Edificios Investigación de Paterna, CSIC - Universitat de València, Apdo. de
Correos 22085, 46071 Valencia, Spain
```

<sup>b</sup>CPPM - Centre de Physique des Particules de Marseille, CNRS/IN2P3 et Université de la Méditerranée, 163 Avenue de Luminy, Case 902, 13288 Marseille Cedex 9, France

<sup>C</sup>GRPHE - Institut universitaire de technologie de Colmar, 34 rue du Grillenbreit BP 50568 - 68008 Colmar, France

<sup>d</sup>INFN - Sezione di Genova, Via Dodecaneso 33, 16146 Genova, Italy

<sup>e</sup> Friedrich-Alexander-Universität Erlangen-Nürnberg, Erlangen Centre for Astroparticle Physics, Erwin-Rommel-Str. 1, D-91058 Erlangen, Germany

f Direction des Sciences de la Matière - Institut de recherche sur les lois fondamentales de l'Univers - Service d'Electronique des Détecteurs et d'Informatique, CEA Saclay, 91191 Gif-sur-Yvette Cedex, France

g Institut d'Investigació per a la Gestió Integrada de Zones Costaneres (IGIC) - Universitat Politècnica de València. C/ Paranimf, 1. E-46730 Gandia, Spain.

<sup>h</sup>FOM Instituut voor Subatomaire Fysica Nikhef, Science Park 105, 1098 XG Amsterdam, The Netherlands

<sup>i</sup>INFN - Sezione di Bari, Via E. Orabona 4, 70126 Bari, Italy

<sup>j</sup>APC - Laboratoire AstroParticule et Cosmologie, UMR 7164 (CNRS, Université Paris 7 Diderot, CEA, Observatoire de Paris) 10, rue Alice Domon et Léonie Duquet 75205 Paris Cedex 13, France

k LAM - Laboratoire d'Astrophysique de Marseille, Pôle de l'Étoile Site de Château-Gombert, rue Frédéric Joliot-Curie 38, 13388 Marseille cedex 13, France

Dipartimento di Fisica dell'Università, Viale Berti Pichat 6/2, 40127 Bologna, Italy
<sup>m</sup>INFN - Sezione di Bologna, Viale Berti Pichat 6/2, 40127 Bologna, Italy

<sup>11</sup>Dipartimento di Fisica dell'Università ?La Sapienza?, P.le Aldo Moro 2, 00185 Roma, Italy

<sup>o</sup>INFN -Sezione di Roma, P.le Aldo Moro 2, 00185 Roma, Italy

P Clermont Université, Université Blaise Pascal, CNRS/IN2P3, Laboratoire de Physique Corpusculaire, BP 10448, F-63000 Clermont-Ferrand, France

<sup>Q</sup>Dipartimento di Fisica dell'Università, Largo B. Pontecorvo 3, 56127 Pisa, Italy

<sup>T</sup>INFN - Sezione di Pisa, Largo B. Pontecorvo 3, 56127 Pisa, Italy

<sup>S</sup>INAF-IASF, via P. Gobetti 101, 40129 Bologna, Italy

<sup>t</sup> Géoazur - Université de Nice Sophia-Antipolis, CNRS/INSU, IRD, Observatoire de la Côte d?Azur and Université Pierre et Marie Curie ? F-06235, BP 48, Villefranche-sur-mer, France

<sup>u</sup>INFN - Laboratori Nazionali del Sud (LNS), Via S. Sofia 62, 95123 Catania, Italy

<sup>V</sup>Direction des Sciences de la Matière - Institut de recherche sur les lois fondamentales de l'Univers - Service de Physique des Particules, CEA Saclay, 91191 Gif-sur-Yvette Cedex, France

<sup>W</sup> COM - Centre d?Océanologie de Marseille, CNRS/INSU et Université de la Méditerranée, 163 Avenue de Luminy, Case 901, 13288 Marseille Cedex 9, France

<sup>X</sup>Université Paris-Sud 11 - Département de Physique - F - 91403 Orsay Cedex, France

<sup>y</sup> IPHC-Institut Pluridisciplinaire Hubert Curien - Université de Strasbourg et CNRS/IN2P3 23 rue du Loess -BP 28-F67037 Strasbourg Cedex 2

<sup>Z</sup>Royal Netherlands Institute for Sea Research (NIOZ), Landsdiep 4,1797 SZ 't Horntje (Texel), The Netherlands

aa Kernfysisch Versneller Instituut (KVI), University of Groningen, Zernikelaan 25, 9747 AA Groningen, The Netherlands

ab Universiteit Utrecht, Faculteit Betawetenschappen, Princetonplein 5, 3584 CC Utrecht, The Netherlands

ac Universiteit van Amsterdam, Instituut voor Hoge-Energie Fysika, Science Park 105, 1098 XG Amsterdam, The Netherlands

ad Dipartimento di Fisica ed Astronomia dell'Università, Viale Andrea Doria 6, 95125 Catania, Italy
ae University of Wisconsin - Madison, 53715, WI, USA

af Institute for Space Sciences, R-77125 Bucharest, Măgurele, Romania

<sup>ag</sup>Dipartimento di Fisica dell'Università, Via Dodecaneso 33, 16146 Genova, Italy

#### **Abstract**

The AMADEUS system described in this article is integrated into the ANTARES neutrino telescope in the Mediterranean Sea and aims at the investigation of techniques for acoustic detection of neutrinos in the deep sea. Installed at water depths between 2000 and 2400 m, its acoustic sensors employ piezo-electric elements for the broad-band recording of signals with frequencies ranging up to 125 kHz with typical sensitivities around -145 dB re. 1V/μPa (including preamplifier). Completed in May 2008, AMADEUS consists of six "acoustic clusters", each comprising six acoustic sensors that are arranged at distances of roughly 1 m from each other. Three acoustic clusters each are installed along two vertical mechanical structures (so-called lines) of the ANTARES detector at a horizontal distance of 240 m. Vertical spacings within a line range from 15 m to 125 m. Each cluster contains custom-designed electronics boards to amplify and digitise the acoustic data from the sensors. The data transmission to shore is done via optical fibres, using the TCP/IP protocol. An on-shore computer cluster, currently consisting of four dedicated servers, is used to process, filter and store the selected data. The daily volume of recorded data is about 10 - 20 GByte. The system is operating continuously and automatically, requiring only little human intervention. AMADEUS allows for extensive studies of both transient signals and ambient noise in the deep sea as well as signal correlations on several length scales and localisation of acoustic point sources. Thus the system is excellently suited to assess the background conditions that affect the measurement of bipolar pulses expected to originate from neutrino interactions. This in turn allows for feasibility studies of a future large-scale acoustic neutrino telescope in the Mediterranean Sea.

Key words: AMADEUS, ANTARES, Neutrino telescope, Acoustic neutrino detection,

Thermo-acoustic model

PACS: 95.55.Vj, 95.85.Ry, 13.15.+g, 43.30.+m

#### 1 Introduction

- 2 The use of acoustic pressure pulses is a promising approach for the detection of
- 3 cosmic neutrinos with energies exceeding 100 PeV in huge underwater acoustic ar-
- 4 rays. The pressure signals are produced by the particle cascades that evolve when
- 5 a neutrino interacts with a nucleus in the water. This energy deposition leads to a

Email address: robert.lahmann@physik.uni-erlangen.de(R. Lahmann).

<sup>\*</sup> Corresponding author

Also at University of Leiden, the Netherlands

On leave at DESY, Platanenallee 6, D-15738 Zeuthen, Germany

local heating of the medium which can be regarded as instantaneous with respect to the hydrodynamic time scale. According to the thermo-acoustic model [1,2], the medium expands or contracts according to its volume expansion coefficient as a result of the temperature change. The accelerated motion of the heated volume forms a pressure pulse of bipolar shape in time—a micro-explosion—which propagates in the surrounding medium. The pulse has a characteristic frequency spectrum that is expected to peak around 10 kHz after propagating several hundreds of metres in 12 sea water in the direction perpendicular to the shower axis [3,4]. Besides sea water, which is the medium under investigation in the case of the AMADEUS 3 project, ice [5] and fresh water [6] are investigated as media for acoustic detection of neutrinos. Studies in sea water are also pursued by other groups using military arrays of underwater microphones (hydrophones) [7,8] or exploiting other existing deep sea infrastructures [9].

Two major advantages over an optical neutrino telescope make acoustic detection worth studying. First, the attenuation length in sea water is of the order of 5 km 20 (1 km) for 10 kHz (20 kHz) signals. This is one to two orders of magnitude larger 21 than for Cherenkov light in the relevant frequency band (attenuation length of the order of 60 m for blue light). Thus the sensor spacings in a potential future large-23 scale acoustic detector are not governed by the attenuation length but instead by 24 the prerequisites set forth by the reconstruction requirements for neutrino events. The second advantage is the much simpler sensor design and readout electronics for acoustic measurements: No high voltage is required and for acoustic signals the time scales are in the µs range, where suitable off-the-shelf electronics is readily 28 available, compared to the ns range for optical signals. This allows the online implementation of advanced signal processing techniques. Efficient data filters are essential, as the signal amplitude is relatively small compared to the acoustic background 31 in the sea, which complicates the unambiguous determination of the signal. Since the sound velocity 4 is small compared to the speed of light, coincidence windows between two separated sensors are correspondingly large. For a high background rate, this can render the reconstruction of signals difficult to impossible if the sensor spacings are too large. To overcome this problem, while at the same time not sacrificing the advantages given by the large attenuation length, AMADEUS uses the concept of several spatially separated *local clusters*. This is described in Sec. 2.

27

34

The AMADEUS project was conceived to perform a feasibility study for a potential future large scale acoustic detector. The project extends the ANTARES detector [10,11] with a dedicated array of acoustic sensors. In the context of AMADEUS the following aims are being pursued:

• Long-term background investigations (rate of neutrino-like signals, spatial and

ANTARES Modules for the Acoustic Detection Under the Sea.

The speed of sound in sea water depends on temperature, salinity and pressure, i.e. depth. A good guideline value for the speed of sound at the location of AMADEUS is 1500 m/s.

- temporal distributions of sources, levels of ambient noise);
- Investigation of correlations for transient signals and for persistent background on different length scales;
- Development and tests of filter and reconstruction algorithms;
- Investigation of different types of acoustic sensors and sensing methods;
- Studies of hybrid (acoustic and optical) detection methods.

Especially the rate and correlation length of neutrino-like acoustic background events, in particular at the ANTARES site, is not known but is a prerequisite for estimating the sensitivity of such a detector.

In this paper, the AMADEUS system within the ANTARES detector is described. In Sec. 2, an overview of the system is given, with particular focus on its integration into the ANTARES detector. In Sec. 3, the system components are described and in Sec. 4, the system performance discussed. The characteristic features of the AMADEUS system are mainly determined by two components: The acoustic sensors and the custom-designed electronics board, which performs the off-shore processing of the analogue data from the acoustic sensors. These two components are discussed in detail in Sections 3.1 and 3.4.

### 61 2 Overview of the AMADEUS System

# 62 2.1 AMADEUS as part of the ANTARES detector

AMADEUS is integrated into the ANTARES neutrino telescope [10] in the Mediterranean Sea, which was designed to reconstruct the tracks of up-going muons originating from neutrino interactions by detecting the Cherenkov light induced by the passage of relativistic charged particles. The ANTARES detector was completed in May, 2008, by the installation of the last components. A sketch of the detector, with the AMADEUS modules highlighted, is shown in Fig. 1. The detector is located at a water depth of about 2500 m, about 40 km south of the town of Toulon on the French Mediterranean coast. It comprises 12 vertical structures, the *Detection* Lines, plus a 13th line, called Instrumentation Line (IL), equipped with instruments 71 for monitoring the environment. Each detection line holds 25 storeys that are ar-72 ranged at equal distances of 14.5 m along the line, starting at an altitude of about 100 m above the sea bed and interlinked by electro-mechanical-optical cables. A standard storey consists of a titanium support structure, holding three Optical Modules [12] (photomultiplier tubes (PMTs) inside water-tight pressure-resistant glass 76 spheres) and one Local Control Module (LCM). The LCM contains the off-shore electronics and a power supply within a cylindrical titanium container (cf. Sec. 3.3). The IL holds six storeys, all of which are non-standard. The vertical distance be-79 tween consecutive storeys is increased to 80 m for two pairs of storeys in the IL.

Each line is fixed on the sea floor by an anchor equipped with electronics and held vertically by an immersed buoy. An interlink cable connects each line to the *Junc-tion Box* from where the main electro-optical cable provides the connection to the shore station.

The ANTARES lines are free to swing and rotate in the undersea currents. In order to determine the positions of the storey with a precision of about 20 cm—as required to achieve the specified pointing precision of reconstructed muon tracks—the detector is equipped with an acoustic positioning system [13]. The system employs an acoustic transceiver at the anchor of each line and up to four autonomous transponders positioned around the 13 lines. Along each detection line, five positioning hydrophones receive the signals of the emitters. By performing multiple time delay measurements and using these to triangulate the individual hydrophones, the line shapes can be reconstructed relative to the positions of the emitters. Currently, the sequence of signal emissions required for the positioning is emitted every 2 minutes.

In AMADEUS, acoustic sensing is integrated in form of *Acoustic Storeys* which are modified versions of standard ANTARES storeys, replacing the OMs by custom-designed acoustic sensors and using dedicated electronics for the digitisation and preprocessing of the analogue signals.

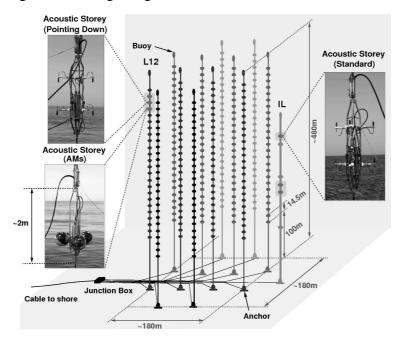


Figure 1. A sketch of the ANTARES detector. The six Acoustic Storeys are highlighted and their three different setups are shown. L12 and IL denote Line 12 and the Instrumentation Line, respectively.

The AMADEUS system comprises a total of six Acoustic Storeys: Three on the IL, which started data taking when the connection to shore of the IL was made in December 2007; and three on Line 12 which were connected to shore during

the completion of the ANTARES detector in May 2008. AMADEUS is now fully functional and routinely taking data with 34 sensors <sup>5</sup>.

The Acoustic Storeys on the IL are located at 180 m, 195 m, and 305 m above the 105 sea floor. On Line 12, which is anchored at a horizontal distance of about 240 m 106 from the IL, the Acoustic Storeys are positioned at heights of 380 m, 395 m, and 107 410 m above the sea floor. With this setup, the maximum distance between two 108 Acoustic Storeys is 340 m. AMADEUS hence covers three length scales: spacings of the order of 1 m between sensors within a storey forming a cluster; intermediate distances of about 15 m between adjacent Acoustic Storeys within a line; and large 111 scales from about 100 m vertical distance on the IL up to 340 m between storeys on 112 different lines. The sensors within a cluster allow for triggering and for direction 113 reconstruction; the directional reconstruction from different Acoustic Storeys can 114 then be combined for the position reconstruction of acoustic sources [14]. The system has full detection capabilities—including time synchronisation and a continuously operating system for long-term data acquisition—and is scalable to a larger number of Acoustic Storeys.

### e 2.2 Acoustic Storeys

Two types of sensing devices are used in AMADEUS: hydrophones and *Acoustic Modules* (AMs). The sensors are in both cases based on the piezo-electric effect and are discussed in Sec. 3.1. Figure 2 shows the design of a standard Acoustic Storey with hydrophones.

The three Acoustic Storeys on the IL house hydrophones only, whereas the lower-most Acoustic Storey of Line 12 holds AMs (cf. Fig. 3(a)). In the central Acoustic Storey of Line 12, the hydrophones were exceptionally mounted to point down-wards (cf. Fig. 3(b)), largely reducing the upwardly sensitivity. This allows for investigating the directionality of background from ambient noise, which is expected to come mainly from the sea surface.

Three of the five storeys holding hydrophones are equipped with commercial models, dubbed "HTI hydrophones <sup>6</sup>", and the other two with hydrophones developed and produced at the Erlangen Centre for Astroparticle Physics (ECAP), described in detail in Sec. 3.1.

<sup>&</sup>lt;sup>5</sup> Two out of 36 hydrophones became inoperational during the initial deployment. No further deterioration of the performance has been observed since then.

<sup>&</sup>lt;sup>6</sup> Custom produced by High Tech Inc (HTI) in Gulfport, MS (USA).

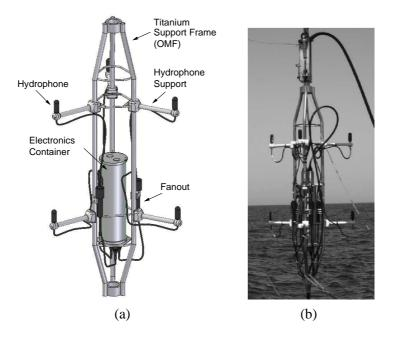


Figure 2. (a) Drawing of a standard Acoustic Storey with hydrophones; (b) photograph of a standard storey during deployment (central Acoustic Storey on the Instrumentation Line).

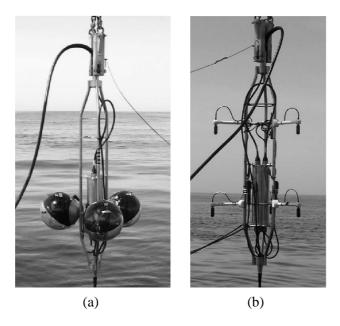


Figure 3. Photographs of the two non-standard storeys of the AMADEUS system during their deployment: (a) The lower-most Acoustic Storey on Line 12 equipped with Acoustic Modules; (b) the central Acoustic Storey on Line 12 with the hydrophones pointing down.

# 2.3 Design Principles

A fundamental design guideline for the AMADEUS system has been to use existing ANTARES hard- and software as much as possible. In this way the design efforts

were kept to a minimum and new quality assurance and control measures had to be introduced only for the additional components, which were subjected to an intensive testing procedure. The high water pressure of up to 250 bar and the salinity of the water constitute a hostile environment that imposes strong requirements on the material of the detector.

In order to integrate the AMADEUS system into the ANTARES detector, design and development efforts in the following basic areas were necessary:

- The development of acoustic sensing devices that replace the Optical Modules of standard ANTARES storeys and of the cables to route the signals into the electronics container;
- The development of an off-shore acoustic digitisation and preprocessing board;
- The setup of an on-shore server cluster for the online processing of the acoustic data and the development of the online software;
  - The development of offline reconstruction and simulation software.

Six acoustic sensors per storey were implemented. This number was the maximum compatible with the design of the LCM and the bandwidth of data transmission to shore. Furthermore, the length of the hydrophone supports (cf. Fig. 2) was chosen to not exceed the diameter of the spheres of the Optical Modules, hence assuring compatibility with the deployment procedure of the ANTARES lines.

# 6 2.4 The AMADEUS-0 Test Apparatus

In March 2005, a full-scale mechanical prototype line for the ANTARES detector was deployed and subsequently recovered [15] for leak-testing the titanium LCM containers and investigating the behaviour of the inter-storey electro-optical cable and its connectors under pressure. This line, dubbed *Line 0*, contained no photomultipliers and no readout electronics. Instead, a miniature autonomous data logging system and shore-based optical time-domain reflectometry were used to record the status of the setup.

Line 0 provided a well-suited environment to study the properties of the acoustic 164 sensors in-situ at a time when the readout electronics for AMADEUS was still in 165 the planning phase and the piezo-preamplifier setup in the design phase. For this 166 purpose, an autonomous system within a standard LCM container, the AMADEUS-167 0 device, was integrated into Line 0. It recorded acoustic noise at the ANTARES site using five piezo sensors with custom-designed preamplifiers, glued to the inside 169 of the LCM container. A battery-powered readout and data logging system was 170 devised and implemented using commercially available components. The system 171 was further equipped with a timing mechanism to record data over two pre-defined 172 periods: The first one lasted for about 10 hours and included the deployment of 173 the line. During this period, a total of 2:45 hours of data were taken over several

intervals. In the second period, with the line installed on the sea floor, 1:45 hours of data were taken over a period of 3:30 hours until the battery power was exhausted.

The analysis of the data [16] provided valuable information for the design of the AMADEUS system. In particular, the level of the recorded noise allowed for tuning the sensitivity and frequency response of the preamplifiers and amplifiers of the AMADEUS system.

# 181 3 System Components

#### 3.1 The Acoustic Sensors

The fundamental components of both the hydrophones and the Acoustic Modules are piezo-electrical ceramics, converting pressure waves into voltage signals [17], and preamplifiers. A schematic view of an ECAP hydrophone is shown in Fig. 4. For these hydrophones <sup>7</sup> two-stage preamplifiers were used: Adapted to the capacitive nature of the piezo elements and the low induced voltages, the first preamplifier stage is charge integrating while the second one is amplifying the output voltage of the first stage. The shape of the ceramics is that of a hollow cylinder.

Due to hardware constraints of the electronics container, the only voltage available for the operation of the hydrophone preamplifiers was 6.0 V. In order to minimise electronic noise, the hydrophone preamplifiers was designed for that voltage rather than employing DC/DC converters to obtain the 12.0 V supply more typically used.

The piezo elements and preamplifiers of the hydrophones are coated in polymer plastics. Plastic endcaps prevent the material from pouring into the hollow part of the piezo cylinder during the moulding procedure. All hydrophones have a diameter of 38 mm and a length (from the cable junction to the opposite end) of 102 mm. The hydrophones produced at ECAP were designed to match the dimensions of the sensors ordered from HTI.

The equivalent inherent noise level in the frequency range from 1 to 50 kHz is about 13 mPa for the ECAP hydrophones and about 5.4 mPa for the HTI hydrophones.

This compares to 6.2 mPa of the lowest expected ambient noise level in the same frequency band for a completely calm sea [18].

At the ANTARES site, the hydrophones are subject to an external pressure of 200 – 240 bar. Prior to deployment, each hydrophone was pressure-tested in accordance

<sup>&</sup>lt;sup>7</sup> For the commercial hydrophones, details were not disclosed by the manufacturer, but the main design is similar to the one described here.

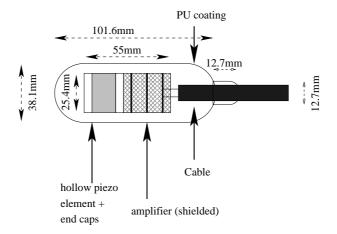


Figure 4. Schematic view of an ECAP hydrophone. Piezo and preamplifier are moulded into polyurethane (PU).

with ANTARES rules, i.e. the pressure was ramped up to 310 bar at 12 bar per minute, held there for two hours and then ramped down again at 12 bar per minute.

For the AMs, the same preamplifiers are used as for the ECAP hydrophones. The piezo elements have the same outer dimensions but in the shape of a solid cylinder. Two sensors are glued to the inside of each of the spheres normally used for the Optical Modules of the ANTARES detector. This design was inspired by the idea to investigate an option for acoustic sensing that can be combined with a PMT in the same housing. In order to assure an optimal acoustic coupling, the space between the curved sphere and the flat end of the piezo sensor of the AM was filled with epoxy. A photograph of an Acoustic Module and a schematic drawing of the sensors glued to the inside of the glass sphere are shown in Fig. 5.

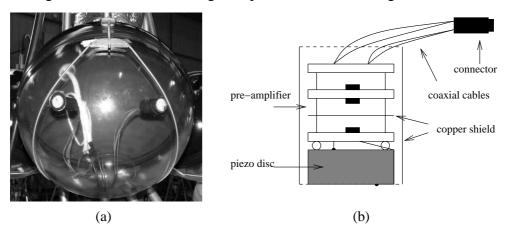


Figure 5. (a) Photograph of an Acoustic Module (AM) before deployment; (b) schematic drawing of an AM sensor.

In order to obtain a complete  $2\pi$ -coverage of the azimuthal angle  $\phi$ , the 6 sensors are distributed over the three AMs of the storey within the plane defined by the three nominal centres of the spheres. The two sensors in each sphere are separated by an angle of  $60^{\circ}$  with respect to the centre of the sphere. The sphere has an outer

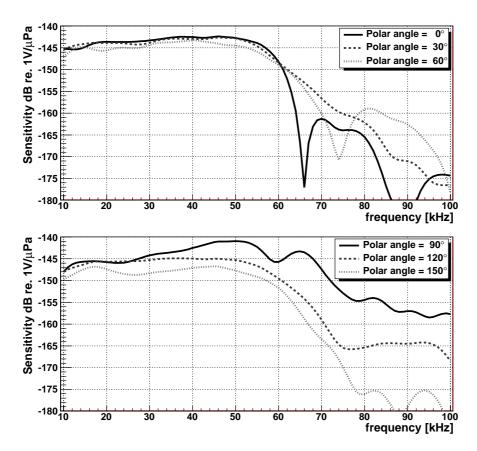


Figure 6. Typical sensitivity of an HTI hydrophone as a function of frequency for different polar angles.

All sensors are tuned to have a low noise level and to be sensitive over the frequency range from 1 to  $50\,\mathrm{kHz}$  with a typical sensitivity around  $-145\,\mathrm{dB}$  re.  $1V/\mu\mathrm{Pa}$  (including preamplifier). The sensitivity of one of the commercial hydrophones is shown in Fig. 6 as a function of frequency for different polar angles [19]. For frequencies below  $50\,\mathrm{kHz}$ , the sensitivity decreases once the polar angle approaches  $180^\circ$ , which defines the direction at which the cable is attached to the hydrophone. The beginning of this trend can be seen for the polar angle of  $150^\circ$ .

The sensitivity as a function of the azimuthal angle for a given frequency is essentially flat at the 3 dB level. The sensitivity as a function of solid angle and frequency shows no significant deviations between different HTI hydrophones in the frequency range from 10 to  $50 \, \text{kHz}$ . The variations for the hydrophones produced at ECAP are larger, at a level of  $3-4 \, \text{dB}$ .

Each acoustic sensor requires a total of four leads for individual power supply and differential signal readout. In order to connect two hydrophones to one of the three connectors in the electronics container, special *fanout cables* were produced (cf. Fig. 2). For the connection to the SubConn<sup>8</sup> connector sockets of the electronics container, the same mating connector plugs as for the OMs—with redefined pin assignments—were used.

At the other end of the cable, a bulkhead connector AWQ-4/24 of the ALL-WET split series by Seacon <sup>9</sup> was moulded. Each bulkhead connector fans out into six wedge-shaped sectors, into two of which the mating 4-pin connectors, moulded to a neoprene cable with the hydrophone, are inserted. The remaining four sectors of the bulkhead connector are sealed with blind plugs. All 15 fanout cables used within AMADEUS are functioning as expected.

The standard cables used in the ANTARES detector between the electronics container and the OMs are also used to connect the AMs to the LCM with the pinning redefined to match that for the hydrophones. The LCMs integrated into storeys with AMs and with hydrophones are equivalent.

# 51 3.3 Off-Shore Electronics

259

260

263

In the ANTARES data acquisition (DAQ) scheme [20], the digitisation is done within the off-shore electronics container (cf. Sec. 2). Each LCM contains a back-plane that is equipped with the connectors for the electronics cards and provides power and data lines to and from the connectors. A standard LCM for processing the data from PMTs contains the following electronics boards:

- Three *ARS motherboards* comprising two Analogue Ring Sampler (ARS) ASICs each for conditioning and digitisation of the analogue data from the PMTs [21];
  - A DAQ board, which reads out the ARS motherboards and handles the communication to the shore via TCP/IP;
- A *Clock board* that provides the timing signals to correlate measurements performed in different storeys (cf. Sec. 3.6).
  - A Compass board that measures the tilt and the orientation of the storey.

The transmission of data to shore is done through Master LCMs (MLCMs) which—in addition to the components of an LCM described above—contain an Ethernet

<sup>&</sup>lt;sup>8</sup> MacArtney Underwater Technology group, http://www.subconn.com.

<sup>&</sup>lt;sup>9</sup> Seacon (Europe) LTD, Great Yarmouth, Norfolk, UK. Seacon also manufactured the fanout cables.

Switch and additional boards for handling incoming and outgoing fibre-based optical data transmission. Up to five storeys form a sector, for which the individual LCMs transmit the data to the MLCM.

For the digitisation of the acoustic signals and for feeding them into the ANTARES data stream, the *AcouADC board* was designed. They are pin-compatible with the ARS motherboards and replace those in the Acoustic Storeys. Figure 7 shows the fully equipped LCM of an Acoustic Storey.

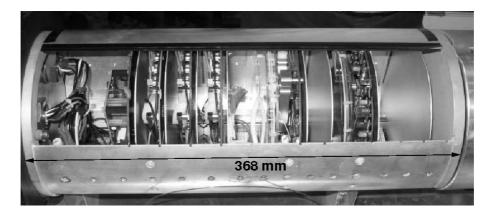


Figure 7. An LCM equipped with AcouADC boards before insertion into its titanium housing. From left to right, the following boards are installed: a Compass board; three AcouADC boards; a DAQ board; a Clock board.

#### гз 3.4 The AcouADC Board

The AcouADC board has the following major tasks:

- Preprocessing of the analogue data for the digitisation (impedance matching, application of an anti-alias filter, selectable gain adjustment) for two acoustic sensors;
- Digitisation of the analogue data and preparation of the digitised data stream for the serial transmission to the DAQ-board;
- Provision of two stable low-noise voltage lines (6V) for the power supply of two hydrophones;
- Provision of an interface to the on-shore control software to set the run parameters (cf. Sec. 3.5).

A photograph and a block diagram of an AcouADC board are shown in Figs. 8 and 9, respectively. The board consists of an analogue and a digital part. Each board processes the differential voltage signals from two acoustic sensors, referred to as "Sig 0" and "Sig 1" in the diagram. The two signals are processed independently and in parallel for the complete (analogue and digital) data processing chain.

A main design criterion for the board was low noise, such that even for a completely calm sea no significant contribution to the recorded noise signal originates from the electronics of the board. To protect the analogue parts from potential electromagnetic interference, they are shielded by metal covers. Tests of the electromagnetic compatibility (EMC) of the board have shown that this design is vulnerable to electromagnetic noise only for conditions that are far more unfavourable than those expected in situ; and even then only at a level that does not significantly affect the acoustic measurements [18].

The two 6V power supply lines on each AcouADC board (connectors labeled "Pow 0" and "Pow 1" in Fig. 9) are protected by resettable fuses against short cicuits that could be produced by the sensors due to water ingress. In addition, each voltage line can be individually switched on or off.

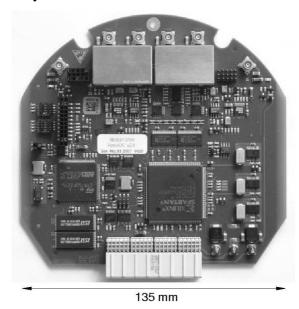


Figure 8. An AcouADC board. The four connectors for the two differential input signals are located at the top, the analogue signal processing electronics is covered by metal shields. The two 6V power connectors are located to the left and right of the shields.

### 3.4.1 Analogue Part

In the analogue part each signal is amplified in two stages. The first stage applies a coarse gain with nominal amplification factors of 1, 10 or 100. It is implemented as a differential amplifier with single-ended output, referenced to 2.5 V. The gain factor 1 is used to record dedicated runs of signals with a large amplitude (e.g. from the emitters of the ANTARES acoustic positioning system (cf. Sec. 2.1)), whereas the factor of 100 is a safety feature in case the sensitivity of the hydrophones should drop significantly due to the long-term exposure to the high pressure.

The second amplification stage, the fine gain, is intended to adjust the gains of different types of hydrophones. It is a non-inverting amplification with single ended

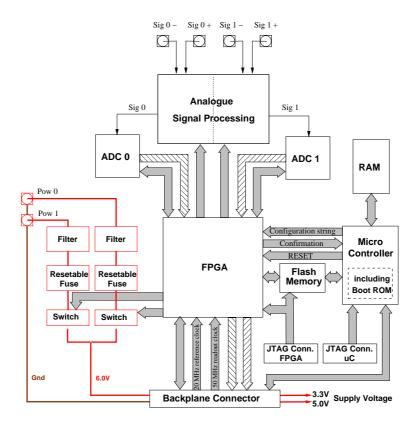


Figure 9. Block diagram of the AcouADC board. The flow of the analogue sensor signals is indicated by thin arrows, hatched arrows denote the flow of the digitised data further downstream. General communication connections are shown as shaded arrows; some signals are denoted by their names. The components relevant for the power supply of the hydrophones are shown in the left part. Voltage supply lines are indicated by thick lines. Connectors are indicated as squares with inlaying circles.

output and a reference voltage of 2.5 V. Gain factors of 1.00, 1.78, 3.16, and 5.62 (corresponding to 0, 5, 10, and 15 dB, respectively) are selectable by switching between four appropriate resistors in the feedback loop of the operational amplifier. Combining the two stages, the gain can be set to one of 12 factors between 1 and 562. The standard setting is an overall gain factor of 10.

After amplification in the two stages described above, the signal is coupled into a linear-phase 10th-order anti-alias filter with a root-raised cosine amplitude response and a 3 dB point at  $f_{\rm cutoff} = 128 \, \rm kHz^{10}$ . In low-power mode, the filter output has a typical maximal point-to-point amplitude of 3.9 V. The output is referenced to 2.0 V and fed into the analogue-to-digital converter (ADC). Accordingly, the ADC reference voltage is set to 2.0 V, implying that the digital output of zero corresponds to this analogue value, with an input range from 0.0 to 4.0 V.

The three analogue stages (coarse and fine amplification and anti-alias filtering) and the ADC are decoupled by appropriate capacitors. Furthermore, several RCL

<sup>&</sup>lt;sup>10</sup> Filter LTC1569-7 from Linear Technology.

elements within the analogue signal chain form an additional band pass filter: A high-pass filter with a 3dB point of about 4 kHz cuts into the trailing edge of the low-frequency noise of the deep-sea acoustic background [22] and thus protects the system from saturation. Additional RCL elements forming passive filters were implemented to comply with the input requirements of active components of the circuitry.

### 3.4.2 Digital Part

The digital part of the AcouADC board digitises and processes the acoustic data. 332 It is highly flexible due to the use of a micro controller  $(\mu C)^{11}$  and a field pro-333 grammable gate array (FPGA)  $^{12}$  as data processor. The  $\mu$ C can be controlled with 334 the on-shore control software and is used to adjust settings of the analogue part and 335 the data processing. Furthermore, the  $\mu$ C can be used to update the firmware of the 336 FPGA in situ. All communication with the shore is done by the μC via the DAQ 337 board. For laboratory operation, JTAG connectors to access the FPGA, μC, and the 338 flash memory are provided. The latter stores the firmware loaded into the FPGA 339 when it is reset. In-situ, the reset is asserted from the  $\mu$ C. If a firmware update is performed, the µC first loads the code from the shore into the random access memory (RAM). Only when the integrity of the code has been confirmed by means of 342 a checksum, the code is transmitted into the flash memory. In order to avoid the 343 potential risk that a software error renders the µC inaccessible, its boot ROM can 344 only be changed in the laboratory. 345

The digitisation is done at 500 kSps (kSamples per second) by one 16-bit ADC <sup>13</sup> for each of the two input channels. The digitised data from the two channels is read out in parallel by the FPGA and further formatted for transmission to the DAQ board.

ADCs do commonly show relatively high deviations from a linear behaviour near the zero point of their digital range. The size of this effect depends on the circuitry into which the ADC is embedded. For the prototypes of the AcouADC boards, this effect proved to be fairly pronounced. For this reason, the reference voltage of the anti-alias filter output can be switched from its standard value of 2.0 V to 1.0 V, thereby moving the peak of the noise distribution away from the digital value of zero.

In standard mode, the sampling rate is reduced to 250 kSps in the FPGA, corresponding to a downsampling by a factor of 2 (DS2). Hence the frequency spectrum of interest from 1 to 100 kHz is fully contained in the data. Currently implemented is a choice between DS1 (i.e. no downsampling), DS2, and DS4, which can be set

<sup>&</sup>lt;sup>11</sup> STR710 from STMicroelectronics.

<sup>&</sup>lt;sup>12</sup> Spartan-3 XC3S200 from XilinX.

<sup>&</sup>lt;sup>13</sup> ADS8323 successive approximation ADC from Analog Devices.

from the shore. Each downsampling factor requires an adapted digital anti-alias filter that is implemented in the FPGA as finite impulse response (FIR) filter with a length of 128 data points.

### 3.4.3 System Characteristics

365

366

367

368

369

371

372

373

374

375

The complex response function of the AcouADC board (i.e. amplitude and phase) was measured in the laboratory prior to deployment for each board and a physically motivated parameterisation of the function was derived [18]. Fig. 10 shows the frequency response of the AcouADC board. The measurement was done by feeding Gaussian white noise into the system and analysing the digital output recorded by the board. Without downsampling (DS1), the rolloff at high frequencies is governed by the analogue anti-alias filter. For DS2 and DS4, the digital FIR filters are responsible for the behaviour at high frequencies. At low frequencies, the effect of the high-pass filter described above can be seen. Fig. 10 shows furthermore that within each passband, the filter response is essentially flat. The comparison of the recorded data with the parameterisation shows excellent agreement.

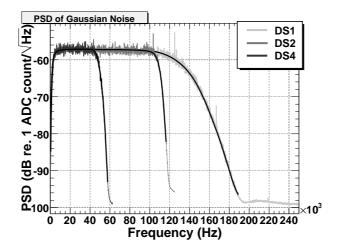


Figure 10. The filter response, characterised as power spectral density (PSD) as a function of the frequency, measured for the three different downsampling factors. For each of the three measurements, the parameterisation is shown as a black line.

Fig. 11 shows a comparison of the measured and calculated response to a bipolar input pulse as it would be expected from a neutrino shower (cf. Sec. 1). The digital FIR filter would introduce an additional time offset of 128 µs of the digitised data for downsampling factors 2 and 4.

The ADCs of the AcouADC board were investigated in detail [18]. For each individual ADC, the transfer curve from input voltage to least significant bits (LSBs) 14

<sup>&</sup>lt;sup>14</sup> The LSB is commonly used to denote one ADC count; the full-scale digital range for a 16-bit ADC is therefore 65535 LSB.

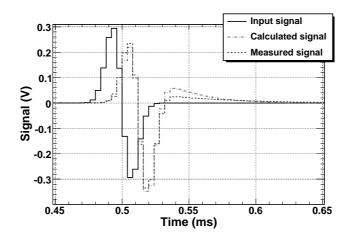


Figure 11. The response of an AcouADC board to a bipolar input pulse. Shown are the measured signal and the signal calculated from the parameterised response function. The measured signal was obtained with an oscilloscope at the input of the ADC. The measurement was done for a nominal gain factor of 1.

was measured and distortions from the ideal linear behaviour quantified in terms of 382 the differential nonlinearity (DNL) and integral nonlinearity (INL). 383

The spurious-free dynamic range (SFDR) of an ADC is defined as the strength ratio of the fundamental signal to the strongest spurious signal in the output and 385 is a measure of the dynamic range of the ADC. Using a sinusoidal input signal, 386 the average SFDR of the ADCs of all boards in AMADEUS was measured to be  $(59.9 \pm 1.1)$  dB, meaning that harmonics of the sine wave distorting the signal are 388 suppressed by 3 orders of magnitude in the amplitude. Hence a clear determina-389 tion of the frequency even for saturated signals—for which typically the harmonic 390 components are enhanced—is possible.

Each individual gain factor for each channel was calibrated and the correction factor 392 for gain 1 was measured to be  $0.95\pm0.01$ . Deviations with respect to this value for 393 the 11 other settings were found to be largest with a level of about 10% for the coarse gain of 100 with no significant dependence on the fine gain factor. 395

The inherent noise of the electronics (output for open signal input) and the cross 396 talk (output for open signal 0 or 1, when the other input is fed with a signal) were 397 confirmed to be negligible in comparison with the characteristics of the acoustic 398 sensors. 399

#### Slow Control System 3.5

384

387

The ANTARES Slow Control (SC) system has two main tasks: It provides the off-401 shore components with initialisation and configuration parameters and it regularly 402 monitors whether the operational parameters are within the specified range. In ad-403

dition, the readout of some instruments for environmental monitoring [23] (which is done at intervals of a few minutes) is polled and sent through the SC interface.

For the AMADEUS system, the following parameters can be set from the shore via the SC system for each acoustic channel individually: one of 12 values for the gain; downsampling factor of 1, 2, or 4 (or no data transmission from the AcouADC board); the power supply for the acoustic sensor can be switched on or off; and the reference voltage of the analogue signal fed into the ADC can be switched between 2.0 V and 1.0 V.

To monitor the environment within each LCM container, a humidity sensor and temperature sensors on several boards are installed. One temperature sensor is placed on each AcouADC board. Values read out by the SC system are stored in one Oracle® database, hosted at the IN2P3 <sup>15</sup> computing centre at Lyon, that is centrally used for all needs of ANTARES and AMADEUS.

# 7 3.6 Data Acquisition and Clock System

AMADEUS follows the same "all data to shore" strategy [20] as the ANTARES neutrino telescope, i.e. all digitised data are transmitted to shore via optical fibres, using the TCP/IP protocol. The data stream from the sender DAQ board is tagged with the IP address of the receiving on-shore server. In the ANTARES control room, the data arrive at a Gigabit switch in exactly the same fashion as the data from the PMTs. At the switch the acoustic data are separated from the optical data and routed to the acoustic server cluster based on the transmitted IP address.

The ANTARES clock system operates separately from the DAQ system, using a different set of optical fibres to synchronise data from different storeys. The system provides a highly stable 20 MHz synchronisation signal, corresponding to a resolution of 50 ns <sup>16</sup>, which is generated by a custom-designed system at the ANTARES control room. The synchronisation of this internal clock with the UTC time of the GPS system is established with a precision of 100 ns.

The synchronisation signal is broadcasted to the off-shore clock boards and from there transmitted further to the FPGA of the AcouADC board. Based on this signal, the data packages sent from the AcouADC board to shore via the DAQ board receive a time stamp which allows an offline correlation of the data from different storeys. The 50 ns resolution of the time stamp corresponds to a resolution of less than 0.1 mm of a sound wave travelling at 1500 m/s in water which far exceeds the

<sup>&</sup>lt;sup>15</sup> Institut National de Physique Nucléaire et de Physique des Particules (France).

<sup>&</sup>lt;sup>16</sup> The much higher precision that is required for the synchronisation of the optical signals from the PMTs is provided by a 256-fold subdivision of the 20 MHz signal in the ARS motherboards.

required precision. Differences in the signal transit times between the shore station and the individual storeys are of the order of  $1 \mu s$  and are small enough that they do not need to be corrected for.

# 40 3.7 On-Shore Data Processing and Run Control

The AMADEUS system is operated with a dedicated run control software that was 441 adapted from the standard ANTARES software called RunControl [20]. The latter 442 is a program with a graphical user interface to control and operate the experiment. 443 It is Java-based and reads the configuration of the individual hard- and software components from the ANTARES database, allowing for an easy adaption to the AMADEUS system. Via the database, the RunControl allows for defining different detector setups which may vary in the specified run parameters or may have 447 individual storeys removed in case of hardware problems. Via the clock system the 448 absolute time of the run start is logged in the database with the aforementioned 449 precision of 100 ns. Events recorded during the run then have a timing precision 450 of 50 ns with respect to the start of the run. The end of a run is reached if either a 451 predefined size or duration of the recorded data has been reached (in which case a new run is started automatically) or the run is stopped by the operator. The data of 453 one AMADEUS run are stored in a single file in root format [24], the typical length 454 of a run is 2 to 5 hours. 455

Even though the DAQ system was not designed to operate multiple RunControl programs in parallel, the system proved flexible enough to handle this situation without interference between the runs of AMADEUS and of the ANTARES neutrino telescope.

For the computing requirements of AMADEUS, a dedicated on-shore computer 460 cluster was installed. It currently consists of four servers, of which two are used for data triggering <sup>17</sup> (2 HP ProLiant DL380 G5 with 2×dual core 3 GHz Intel Xeon 462 5160 and 2×quad core 3 GHz Intel Xeon 5450 processors, respectively). Hence, a 463 total of 12 cores are available to process the data received from the ANTARES GBit 464 switch. One of the remaining two servers is used to write the data to an internal 550 465 GByte disk, while the other server is used to operate the RunControl software and 466 miscellaneous other processes. The latter server also provides remote access to the 467 system via the Internet.

The AMADEUS trigger searches the data by an adjustable software filter; the events thus selected are stored to disk. This way the raw data rate of about 1.5 TB/day is reduced to about 15 GB/day for storage. Currently, three trigger schemes are in operation [25]: A minimum bias trigger which records  $\sim 10 \,\mathrm{s}$  of continuous data

 $<sup>^{17}</sup>$  While this functionality might be more commonly referred to as filter system, it is ANTARES convention to refer to the "on-shore trigger".

every 60 min; a threshold trigger which is activated when the signal exceeds a predefined amplitude; and a pulse shape recognition trigger. For the latter, a cross correlation of the signal with a predefined bipolar signal, as it is expected to be recorded for a neutrino shower, is performed. The trigger condition is met if the output of the cross correlation operation exceeds a predefined threshold. This trigger corresponds to a matched filter for a white noise background.

Both, the threshold and the pulse shape recognition trigger are applied to the indi-479 vidual sensors and are self-adjusting to the ambient noise, implying that all trigger 480 thresholds are defined in terms of a signal to noise ratio. The trigger thresholds are 481 freely adjustable. If one of these two trigger conditions is met, an additional trigger condition is imposed, which requires coincidences of a predefined number of 483 acoustic sensors on each storey. The coincidence window is fixed to the length of 484 about 105 ms of a *frame*, i.e. the structure in which data are buffered off-shore by 485 the DAQ-board before being sent to shore [20]. Currently, the coincidence trigger 486 requires that the threshold or pulse shape recognition trigger conditions have been 487 met for at least four out of six sensors. 488

For reasons stemming from the fact that the ANTARES DAQ system was designed to comply with the nanosecond time scales of an optical neutrino telescope, the coincidence window is not implemented as a sliding window but starts at fixed intervals with respect to the run start. However, given the distances of typically 1 m between sensors within one storey, time delays between signals from a given source are always less then 1 ms. Therefore the number of sources for which the signals extend over two frames, and hence the coincidence trigger may not be activated, is small. The coincidence trigger can be optionally extended to require coincidences between different storeys on the same line. With distances between storeys ranging from about 10 m to 100 m (and delays therefore reaching the order of 10 ms to 100 ms) the coincidence window in this case suppresses signals originating from above or below. This trigger level is currently not enabled.

490

491

492

493

494

496

497

498

499

500

Once the coincidence trigger has fired, the data within a time window are stored. First, a window of  $2.56 \,\mathrm{ms}$  (corresponding to  $640 \,\mathrm{data}$  samples at  $4 \,\mu\mathrm{s}$  sampling time) is defined around the point in time when the trigger condition was met. Then adjacent or overlapping windows are merged. Consequently, data are stored for each sensor within time windows with a length ranging from  $2.56 \,\mathrm{ms}$  to  $\sim 105 \,\mathrm{ms}$ .

The triggers of the AMADEUS system and the main ANTARES optical neutrino telescope are working completely independently. Hence the search for potentially correlated signals does rely on offline analyses.

All components of the AMADEUS system are scalable which makes it very flexible. Additional servers can be added or the existing ones can be replaced by new generation models if more sophisticated trigger algorithms are to be implemented. In principle it is also possible to move parts of the trigger algorithm into the FPGA of the AcouADC board, thereby implementing an off-shore trigger which reduces the size of the data stream sent to shore.

Just like the ANTARES neutrino telescope, AMADEUS can be controlled via the Internet and is currently operated from ECAP. Data are centrally stored and are available remotely as well.

# 8 4 System Performance

AMADEUS is continuously operating and taking data with only a few interventions by the RunControl operator per week. The on-time of each sensor is about 75 to 80% and is defined as the ratio between the time over which the sensor is taking data and the active time of that sensor. Not active were only those times during which the power or data transmission to shore was interrupted due to problems that required a sea operation for maintenance.

The concept of local clusters (i.e. the storeys) is very efficient for fast online processing. By requiring coincident signals from at least four sensors within a storey, the rate of the cross correlation trigger is reduced by a factor of more than 20 with respect to the rate of a single sensor when using the same thresholds.

The parallel operation of two separate RunControl programs for AMADEUS and the main ANTARES neutrino telescope has proven to be very successful. No interference between the two programs has been observed while the two systems can optimise their detection efficiency and respond to potential problems almost independently. At the same time, both systems profit in the same fashion from developments and improvements of the RunControl.

The stability of the system is excellent. This was verified prior to deployment as well as in-situ. It was quantified by observing the mean of the ambient noise distribution as a function of time. In-situ, the 10 s of continuous data recorded every hour with the minimum bias trigger were used for the measurement. The worst observed RMS variation of this value for the first year of operation is less than  $2 \cdot 10^{-5}$  of the full range (65535 LSB or 4.0 V).

Studies of the power spectral density of the ambient noise at the ANTARES site
have been performed using the minimum bias trigger data. The lowest level of
recorded noise in situ was confirmed to be consistent with the intrinsic noise of the
system recorded in the laboratory prior to deployment (cf. Fig. 12). The observed
in-situ noise can be seen to go below the noise level measured in the laboratory
for frequencies exceeding 35 kHz. This is due to electronic noise coupling into the
system in the laboratory that is absent in the deep sea. Above that same frequency,
the intrinsic electronic noise starts to dominate over the mean ambient noise. This

frequency consequently constitutes an upper bound for studies of the ambient noise in the deep sea with AMADEUS.

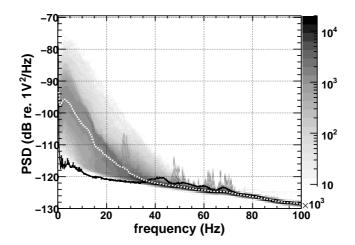


Figure 12. Power spectral density (PSD) of the ambient noise recorded with one sensor on the topmost storey of the IL. Shown in shades of grey is the occurrence rate in arbitrary units, where dark colours indicate higher occurence rates. Shown as a white dotted line is the mean value of the in-situ PSD and as a black solid line the noise level recorded in the laboratory prior to deployment.

Using the same minimum bias data, a further demonstration can be done that the recorded data are indeed representative of the ambient conditions and not determined by the intrinsic noise of the system: the noise levels (i.e. the RMS of the signal amplitudes in each 10 s sample) recorded at the same time with any two active sensors are highly correlated with correlation coefficients between 93% and 100%.

The AMADEUS cross correlation trigger selects signals for which the signal to noise ratio exceeds a value of about 2 for a bipolar signal recorded with a single acoustic sensor. Assuming a noise level of 10 mPa for the frequency range of 1 to 100 kHz, which represents the scale for a combination of the equivalent intrinsic sensor noise and the lowest ambient noise for a calm sea, the corresponding recorded pressure signal would be emitted from a 2 EeV cascade for a neutrino interaction at a distance of 200 m [3]. Using a cross correlation trigger with a signal shape more closely adjusted to the expected signal from a neutrino shower, the energy threshold can be further reduced. This threshold, determined by the ambient noise, is the optimal achievable energy threshold for the detection of neutrinos. The rate at which neutrino-like signals are mimicking neutrino interactions will then set a more stringent limit. This rate is subject to investigation and will be a decisive indication concerning the feasibility of a future large scale acoustic neutrino detector.

The maximal pressure amplitude that can be recorded for a gain factor of 10 without saturating the input range of the ADC is about 5 Pa. Usually only anthropogenic signals originating close to the detector reach this pressure level.

The position reconstruction of acoustic point sources is currently being pursued as one of the major prerequisite to identify neutrino-like signals. Simulation results are presented in [14].

Just as for the standard storeys holding PMTs, the relative positions of the Acoustic Storeys within the detector have to be continuously monitored. This is done by using the emitter signals of the ANTARES acoustic positioning system (cf. Sec. 2.1). Fig. 13 shows such a signal as recorded by four representative sensors. The delays between the signal arrivals are clearly visible: short delays of less than 1 ms within each storey and a long delay of about 10 ms between the signals arriving in two different storeys.

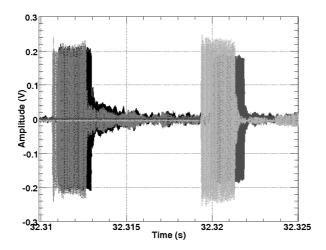


Figure 13. Typical emitter signals of the ANTARES acoustic positioning system as recorded with four sensors of the AMADEUS system. The first two signals along the time axis were recorded by the Acoustic Storey holding AMs (cf. Fig. 1). The following two signals were recorded with two hydrophones on the Acoustic Storey just above—one hydrophone mounted at the bottom and the other one at the top of a storey. All signals were recorded with a gain factor 1 of the AcouADC board. The time is counted since the start of the run.

The time shown in the Figure is given in seconds since the start of the run and can be converted into UTC time using the data recorded by the clock system (cf. Sec. 3.6). As the emission times of the positioning signals are also recorded in UTC time, the time difference between emission and reception of the signal can be calculated. Using the signals from multiple emitters and their known positions at the anchors of the lines, the positions of the AMADEUS sensors can be reconstructed.

The positioning accuracy for each hydrophone shows statistical errors of a few mm for the hydrophones. The final measurement is expected to be dominated by systematic uncertainties due to the physical size of the receiving piezo elements, the knowledge of their relative positions within the acoustic storey, and the knowledge of the speed of sound in sea water. For the AMs, the position reconstruction is less precise and statistical and systematic uncertainties are expected to be of the same

order of magnitude.

As a recent development, marine scientists have become interested in the data recorded by AMADEUS for the study of marine mammals, in particular cetaceans.

The system hence will be used as a multipurpose apparatus for neutrino feasibility studies, acoustic positioning and marine research.

### 5 Summary and Conclusions

The AMADEUS system for the investigation of techniques for acoustic particle detection in the deep sea has been integrated into the ANTARES neutrino telescope in the Mediterranean Sea at water depths between 2000 and 2400 m. The system started taking data in December 2007 and was completed in May 2008. The system consists of 36 acoustic sensors, of which currently 34 are operational, arranged in six acoustic clusters. Different sensor setups and different installations of the acoustic clusters are in operation. The sensors are based on piezo-electric elements and two-stage preamplifiers with combined sensitivities around  $-145 \, dB \, re. \, 1V/\mu Pa$ .

Data sampling is done at 500 kSps with 16 bits and an analogue anti-alias filter with a 3 dB point at  $f_{cutoff} = 128$  kHz. One of twelve steps of analog amplification between 1 to 562 can be set with the on-shore control software. Digital downsampling with factors of 2 and 4 is implemented inside an off-shore FPGA. The value is also selectable using on-shore control software.

All components of the system have been calibrated in the laboratory prior to deployment; the in-situ performance is in full accordance with the expectations. Data taking is going on continuously and the data are recorded if one of three adjustable trigger conditions is met.

The system is well suited to conclude on the feasibility of a future large scale acoustic neutrino telescope in the deep sea. Furthermore, it has the potential of a multi-purpose device, combining its design goal to investigate acoustic neutrino detection techniques with the potential to perform marine science and the ability for positioning. AMADEUS hence is a promising starting point for instrumenting the future neutrino telescope project KM3NeT [26,27] with acoustic sensors for calibration and science purposes.

#### 25 6 Acknowledgments

The authors acknowledge the financial support of the funding agencies: Centre National de la Recherche Scientifique (CNRS), Commissariat à l'Energie Atomique

(CEA), Commission Européenne (FEDER fund and Marie Curie Program), Région Alsace (contrat CPER), Région Provence-Alpes-Côte d'Azur, Département du Var 629 and Ville de La Seyne-sur-Mer, in France; Bundesministerium für Bildung und 630 Forschung (BMBF), grants 05A08WE1, 05A08WEA, and 05CN5WE1/7 in Germany; Istituto Nazionale di Fisica Nucleare (INFN), in Italy; Stichting voor Fun-632 damenteel Onderzoek der Materie (FOM), Nederlandse organisatie voor Weten-633 schappelijk Onderzoek (NWO), in the Netherlands; Russian Foundation for Basic 634 Research (RFBR), in Russia; National Authority for Scientific Research (ANCS) 635 in Romania; Ministerio de Ciencia e Innovación (MICINN), in Spain. We also ac-636 knowledge the technical support of Ifremer, AIM and Foselev Marine for the sea 637 operation and the CC-IN2P3 for the computing facilities.

### 639 References

- [1] G.A. Askariyan, B.A. Dolgoshein et al., Acoustic Detection of High Energy Particle
   Showers in Water, NIM 164 (1979) 267
- [2] J.G. Learned, Acoustic Radiation by Charged Atomic Particles in Liquids: An
   Analysis, PR 19 (1979) 3293
- 644 [3] S. Bevan et al. (ACoRNE Coll.), Simulation of Ultra High Energy Neutrino 645 Interactions in Ice and Water, Astropart. Phys. **28** (2007) 366, arXiv:astro-646 ph/0704.1025v1
- [4] S. Danaher et al. (ACoRNE Coll.), Study of the Acoustic Signature of UHE Neutrino
   Interactions in Water and Ice, arXiv:0903.0949v2 [astro-ph.IM] (2009)
- F. Descamps for the IceCube Coll., Acoustic detection of high energy neutrinos in ice:
   Status and results from the South Pole Acoustic Test Setup, in Proceedings of the 31st
   International Cosmic Ray Conference, (2009), arXiv:0908.3251v2 [astro-ph.IM]
- K. Antipin et al.(BAIKAL Coll.), A prototype device for acoustic neutrino detection in
   Lake Baikal, in Proceedings of the 30th International Cosmic Ray Conference, (2007),
   arXiv:0710.3113 [astro-ph]
- J. Vandenbroucke, G. Gratta and N. Lehtinen, Experimental Study of Acoustic
   Ultra-high-Energy Neutrino Detection, Astrophys. J. 621 (2005) 301, arXiv:astro-ph/0406105
- S. Danaher for the ACoRNE Coll., First Data from ACoRNE and Signal Processing
   Techniques, in Proceedings of ARENA 2006 Acoustic and Radio EeV Neutrino
   detection Activities, J. Phys. Conf. Ser. 81 (2007) 012011
- NEMO Coll., NEMO-OνDE: a submarine station for real-time monitoring of acoustic
   background installed at 2000 m depth in the Mediterranean Sea, submitted to Deep
   Sea Research I, arXiv:0804.2913v1 [astro-ph] (2008)
- 664 [10] The ANTARES Collaboration, *The ANTARES Neutrino Telescope in the*665 *Mediterranean Sea*, to be submitted to NIM A

- [11] M. Ageron et al. (ANTARES Coll.), Performance of the First ANTARES Detector
   Line, Astropart. Phys. 31 (2009) 277, arXiv: 0812.2095 v1 [astro-ph]
- [12] P. Amram et al. (ANTARES Coll.), *The ANTARES optical module*, NIM A 484 (2002)
   369
- 670 [13] M. Ardid for the ANTARES Coll., *Positioning system of the ANTARES neutrino* 671 *telescope*, NIM **A 602** (2009) 174
- [14] C. Richardt et al., Reconstruction methods for acoustic particle detection in the deep sea using clusters of hydrophones, Astropart. Phys. **31** (2009) 19, arXiv:0906.1718v1 [astro-ph.IM]
- [15] M. Ageron et al. (ANTARES Coll.), Studies of a full-scale mechanical prototype line
   for the ANTARES neutrino telescope and tests of a prototype instrument for deep-sea
   acoustic measurements, NIM A 581 (2007) 695
- [16] F. Deffner,
   Studie zur akustischen Neutrinodetektion: Analyse und Filterung akustischer Daten
   aus der Tiefsee, Diploma Thesis, Univ. Erlangen-Nürnberg, (2007, FAU-PII-DIPL-07-001, obtainable from http://www.antares.physik.uni-erlangen.de/publications)
- [17] G. Anton et al. *Study of piezo based sensors for acoustic particle detection*, Astropart. Phys. **26** (2006) 301
- [18] K. Graf, Experimental Studies
   within ANTARES towards Acoustic Detection of Ultra-High Energy Neutrinos in the
   Deep Sea, Doctoral Thesis, Univ. Erlangen-Nürnberg, (2008, FAU-PII-DISS-08-001,
   obtainable from http://www.antares.physik.uni-erlangen.de/publications)
- [19] C.L. Naumann, Development of Sensors for the Acoustic Detection of Ultra High
   Energy Neutrinos in the Deep Sea,
   Doctoral Thesis, Univ. Erlangen-Nürnberg, (2007, FAU-PI4-DISS-07-002, obtainable
   from http://www.antares.physik.uni-erlangen.de/publications)
- [20] J.A. Aguilar et al. (ANTARES Coll.), The data acquisition system for the ANTARES
   neutrino telescope, NIM A 570 (2007) 107
- [21] The ANTARES Collaboration, Performances of the front-end electronics of the ANTARES neutrino telescope, to be submitted to NIM A
- [22] R.J. Urick, *Principles of Underwater Sound* (Peninsula publishing, Los Altos, USA,
   1983)
- [23] J.A. Aguilar et al. (ANTARES Coll.), First results of the Instrumentation Line for the
   deep-sea ANTARES neutrino telescope, Astropart. Phys. 26 (2006) 314
- 700 [24] The root homepage, http://root.cern.ch/
- [25] M. Neff, Studie zur akustischen Teilchendetektion im Rahmen des ANTARES Experiments: Entwicklung und Integration von Datennahmesoftware, Diploma
   Thesis, Univ. Erlangen-Nürnberg, (2007, FAU-PI1-DIPL-07-003, obtainable from
   http://www.antares.physik.uni-erlangen.de/publications)

- [26] U.F. Katz et al. (KM3NeT Consortium), Status of the KM3NeT project, NIM A 602
   (2009) 40
- [27] KM3NeT Consortium, Conceptual Design for a Deep-Sea Research Infrastructure
   Incorporating a Very Large Volume Neutrino Telescope in the Mediterranean Sea,
   ISBN 978-90-6488-031-5, 2008, http://www.km3net.org/CDR/CDR-KM3NeT.pdf